American Journal of Computation, Communication and Control
2015; 2(4): 33-39
Published online January 21, 2016 (http://www.aascit.org/journal/ajccc)
ISSN: 2375-3943

American Association for Science and Technology

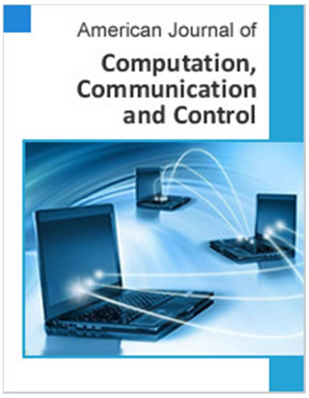

A Vibration Suppression Device of Single-Link Flexible Manipulator and Its Control Algorithm

An Kai

Shandong Aerospace Electro-technology Institute, Yantai, China

Email address
ankai2007@163.com

Citation
An kai. A Vibration Suppression Device of Single-Link Flexible Manipulator and Its Control Algorithm. *American Journal of Computation, Communication and Control.*
Vol. 2, No. 4, 2015, pp. 33-39.

Keywords
Manipulator,
Vibration,
Suppression,
Device,
Control

Received: December 15, 2015
Revised: December 26, 2015
Accepted: December 28, 2015

Abstract
A device which comprises three parts, electromotor, screw and cable, is proposed to suppress the vibration of a single-link flexible manipulator. The manipulator acted on jointly by the device and the load at manipulator's end-effector is modeled as a cantilever beam with three concentrated loads at two end-points and midpoint. By taking the exserted length of the screw as control variable, the curve equation of the cantilever beam is educed. According to the curve equation, the expression about the exserted length of the screw and the maximal offset of the manipulator arm are given in the case of offset at manipulator's end-effector to be zero. By comparing the maximal offset with that in case without using the device, the result shows that the maximal offset in latter case is $3\sqrt{5}$ times. A simulation result shows the shape of manipulator acted on jointly by the device and the load at manipulator's end-effector, and confirms feasibility of the device and its control algorithm. A prominent predominance of the vibration suppression device and its control algorithm is that the maximal offset appears at the midpoint neighborhood of manipulator, but offset at manipulator's end-effector closes to zero.

1. Introduction

Space manipulators are complex systems, composed by robotic arms accommodated on an orbiting platform. They can be used to perform a variety of tasks: launch of satellites, retrieval of spacecraft for inspection, maintenance and repair, movement of cargo and so on [1]. Space missions and on-orbit tasks will rely increasingly on space manipulators, since these tasks are either too risky or very costly, due to safety support systems, or just physically impossible to be executed by humans. All these missions require extreme precision. However, in order to respect the mass at launch requirements, manipulators arms are usually very light and flexible, and their motion involves significant structural vibrations, especially after a grasping maneuver.

Considerable work has been carried out in the vibration suppression of flexible manipulators by various researchers [2-4]. The traditional approaches to minimize the effect of structural vibrations are focused on either increasing the structural stiffness, which increases the system's size and weight, or using closed-loop control methods for active vibration control, which require advanced instrumentation and control equipment that increase the system cost and complexity [5]. Ref. 6 presents the analytic and experimental development of piezoelectric actuators as elements of intelligent structures, i.e., structures with highly distributed actuators, sensors, and processing networks. Static and dynamic analytic models are derived for segmented piezoelectric actuators that are either bonded to an elastic substructure or embedded in a laminated composite. These models lead to the ability to predict, a priori, the response of the structural member to a command voltage applied to the piezoelectric and give guidance as to the optimal location for actuator placement. A scaling analysis is performed to demonstrate that the effectiveness of piezoelectric actuators is independent of the size of the structure and to evaluate various piezoelectric materials based on their effectiveness in transmitting strain to the substructure. Three test specimens of cantilevered beams were constructed: an aluminum beam with surface-bonded actuators, a glass/epoxy beam with embedded actuators, and a graphite/epoxy beam with embedded actuators. The actuators were used to excite steady-state resonant vibrations in the cantilevered beams. The response of the specimens compared well with those predicted by the analytic models. Static tensile tests performed on glass/epoxy laminates indicated that the embedded actuator reduced the ultimate strength of the laminate by 20%, while not significantly affecting the global elastic modulus of the specimen. Ref.7 describes an approach for the use of smart materials, specifically, piezoelectric materials (PZT), in control of a single-link flexible manipulator. It is investigated by a Lyapunov approach that a combined scheme of PD feedback and command voltages applied to segmented PZT actuators, which are bonded to the surface of the flexible link, can effectively control the rigid body motion and at the same time, damp link vibrations. The unique features of the proposed PZT actuator control are twofolds: First, it utilizes linear in contrast to angular velocities of particular points on the link, signals which are readily available. Second, the actuator placement is examined based on the analysis of mode shape functions. Stability of the system with the proposed PZT actuator control is analyzed using a virtual joint model. The shape control of beams by piezoelectric actuators is addressed analytically in [8]. Solutions are presented for a beam subjected to different boundary conditions. The solutions show how and how much the piezoelectric actuators can influence the shape of a beam. Several case studies are also presented to show the applications of the analytical solutions in the various analyses relevant to shape control of beams by piezoelectric actuators. The limitation of the actuation forces produced by piezoelectric actuators makes it difficult to realize global and local precise shape control. Ref. 9 presented and discussed the results of several tests concerning possible application of piezoelectric elements to reduce torsional vibrations of a beam. The piezoelectric elements are positioned in two pairs and glued to the beam at the chosen cross-section. These elements are activated using a harmonically varying voltage of the same amplitude and opposite in phase. Simulations are performed regarding the active reduction of the lowest natural frequencies of vibration of the fixed-free beam with the use of piezoelectric actuators.

However, since the length of a manipulator arm may attain several meters, or even exceed ten meters, the PZT bonded to the surface of the flexible manipulator arm will be either too weightily or very costly. Although some PZT actuators can be bonded to the surface of the arm dividually for reducing weight and cost, it is still a fatal weakness for the maximal offset of the manipulator arm appears at end-effector. The positioning precision of the manipulator is actually the one at end-effector, and hence a desired vibration suppression effect is certainly that the maximal offset of the arm appears at other part except at end-effector. This paper aims at designing and studying active damping strategies and relevant devices that could be used to reduce the structural vibrations of a space manipulator with flexible links during its on orbit operations.

2. Structure and Working Principle of the Vibration Suppression Device

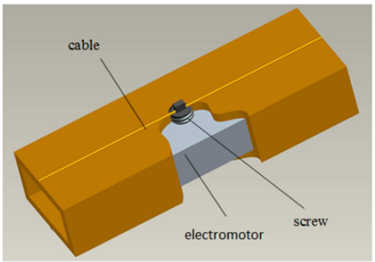

Fig. 1. *Sketch of a vibration suppression device.*

The vibration suppression device comprises three parts, electromotor, screw and cables, as shown in Fig.1. The electromotor, whose axis is a hollow column with internal thread, is mounted on the middle part of the manipulator arm, and can rotate clockwise and counterclockwise. There is a square prism with hole at each end of the screw, and the screw thread of the screw can mesh with internal thread of the hollow axis of the electromotor. Two cables are mounted on two opposite surfaces of the manipulator arm, and their ends are fixed at ends of the arm after the cables cut through the holes in square prisms.

The projection of the load inertial force on the direction perpendicular to plane containing the cables can be obtained by estimating the mass of load and the position of the end-effector, and the contrary direction is the desired movement direction of the screw for vibration suppression. In the following sections a formula to compute the desired protruded length of the screw will be derived using Hooke's law. By controlling the screw's movement according to the above direction and distance, the bending-moment of the manipulator arm coming from inertial force of the load will be counteracted by the bending-moment of a cable, and the purpose of vibration suppression will be achieved accordingly.

3. Curve Equation of the Manipulator Arm

Under the action of the vibration suppression device, the single-link flexible manipulator grasping a payload can be modeled as a uniform cantilever beam shown in Fig. 2, where $L/2$ denotes the distance from screw to tips of the beam, l denotes the length of the screw, P denotes the support force of the screw acting on a cable, R denotes the tensile stress of the cable, R_A and R_B are reactions of P at the support A and B respectively, F denotes the projection of the load inertial force on the direction perpendicular to plane containing the cables, we have

$$R_A = R_B = \frac{P}{2}$$

We now cut through the beam at a cross section to the left of the support force P and at distance x from the support at A. From the equations of equilibrium for this free body, we obtain the bending moment $M(t)$ at distance x from the support A (counterclockwise moments are positive) [10-13]:

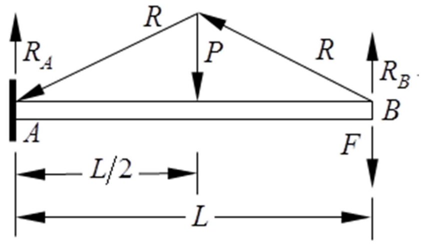

Fig. 2. Cantilever beam with two concentrated loads.

$$M(x) = -(\frac{L}{2} - x)P + (R_B - F)(L - x)$$

$$= (P - R_B + F)x + (R_B - F - \frac{P}{2})L$$

$$= (\frac{P}{2} + F)x - FL \ (0 \le x \le L/2)$$

This expression is valid only for the part of the beam to the left of the support force P.

Next, we cut through the beam to the right of the support force P (that is, in the region $L/2 \le x \le L$). From the equations of equilibrium for this free body, we obtain the following expressions for the bending moment [14]:

$$M(x) = (R_B - F)(L - x) = -(\frac{P}{2} - F)x + (\frac{P}{2} - F)L$$

Note that this equation is valid only for the right-hand part of the beam.

According to the theory of mechanics of materials, the curvature κ of the beam is directly proportional to the bending moment $M(t)$ and inversely proportional to the quantity EI, which is called the flexural rigidity of the beam, and therefore we have the following moment-curvature equation:

$$\kappa = M/EI$$

For reference purposes, we construct a system of coordinate axes whose origin is at the fixed support A, positive x axis is directed to the right, and positive y axis is directed upward, so that the two axes form a right-handed coordinate system. According to the expression of the curvature from differential geometry we get

$$\kappa = \frac{y''}{(1 + y'^2)^{\frac{3}{2}}}$$

In practical application, comparing with its length, the distortion of manipulator arm caused by the bending moment is very small quantity, and the angle of rotation θ whose tangent is equal to y' is accordingly a very small quantity. Therefore, y' may be approximated as zero, and the curvature can be expressed as $\kappa = y''$. Thus, in the case of $0 \le x \le L/2$ we have

$$y'' = \frac{(\frac{P}{2} + F)x - FL}{EI}$$

By using boundary conditions $y(0) = 0$ and $y'(0) = 0$, successive integrations of the last equation yield

$$y = \frac{(P + 2F)}{12EI}x^3 - \frac{FL}{2EI}x^2$$

Taking the derivative of this expression with respect to x, we get

$$y' = \frac{(P + 2F)}{4EI}x^2 - \frac{FL}{EI}x$$

Substituting $x = L/2$ into the last two equations, we find

$$y(\frac{L}{2}) = (P - 10F)\frac{L^3}{96EI} \quad (1)$$

$$y'(\frac{L}{2}) = \frac{(P + 2F)}{16EI}L^2 - \frac{F}{2EI}L^2 = (P - 6F)\frac{L^2}{16EI} \quad (2)$$

In the case of $L/2 \le x \le L$ we have

$$y'' = \frac{-(\frac{P}{2} - F)x + (\frac{P}{2} - F)L}{EI}$$

Integrating the last equation gives

$$y' = -\frac{(P - 2F)}{4EI}x^2 + \frac{(P - 2F)L}{2EI}x + c_1$$

where c_1 is integration constant. Substituting Eq.(2) into the last equation, we find

$$(P-6F)\frac{L^2}{16EI}=-\frac{(P-2F)}{16EI}L^2+\frac{(P-2F)}{4EI}L^2+c_1$$

or

$$c_1=-\frac{PL^2}{8EI}$$

Therefore, the derivative y' is

$$y'=-\frac{(P-2F)}{4EI}x^2+\frac{(P-2F)L}{2EI}x-\frac{PL^2}{8EI}$$

Integrating the last equation gives

$$y=-\frac{(P-2F)}{12EI}x^3+\frac{(P-2F)L}{4EI}x^2-\frac{PL^2}{8EI}x+c_2$$

where c_2 is integration constant. Substituting Eq.(1) into the last equation, we find

$$(P-10F)\frac{L^3}{96EI}=-\frac{(P-2F)}{96EI}L^3+\frac{(P-2F)}{16EI}L^3-\frac{P}{16EI}L^3+c_2$$

$$c_2=\frac{PL^3}{48EI}$$

Therefore, we get

$$y=-\frac{(P-2F)}{12EI}x^3+\frac{(P-2F)L}{4EI}x^2-\frac{PL^2}{8EI}x+\frac{PL^3}{48EI}$$

Combining the equation with Eq.(1), we get the following curve equation of the manipulator arm

$$y(x)=\begin{cases}\frac{(P+2F)}{12EI}x^3-\frac{FL}{2EI}x^2 & 0\le x\le L/2\\ -\frac{(P-2F)}{12EI}x^3+\frac{(P-2F)L}{4EI}x^2-\frac{PL^2}{8EI}x+\frac{PL^3}{48EI} & L/2\le x\le L\end{cases} \quad (3)$$

Substituting $x=L$ into Eq.(31), we find

$$y(L)=-\frac{(P-2F)}{12EI}L^3+\frac{(P-2F)}{4EI}L^3-\frac{PL^3}{8EI}+\frac{PL^3}{48EI}=\frac{(3P-16F)}{48EI}L^3 \quad (4)$$

4. Protruded Length of the Screw

In order to eliminate position offset at manipulator arm's end-effector, equating the right-hand side of Eq.(4) to zero we have $P=\frac{16}{3}F$.

In order to compute the desired protruded length l of the screw, we denote the modulus of elasticity of the cables and its area of cross section by E_0 and S respectively. The elongation of the cables can be expressed as

$$\sqrt{l^2+(L/2)^2}-L/2$$

and the tensile forces in the cables can be expressed as

$$T=SE_0\left(\frac{\sqrt{l^2+(L/2)^2}-L/2}{L/2}\right)=SE_0\left(\sqrt{1+4(\frac{l}{L})^2}-1\right)$$

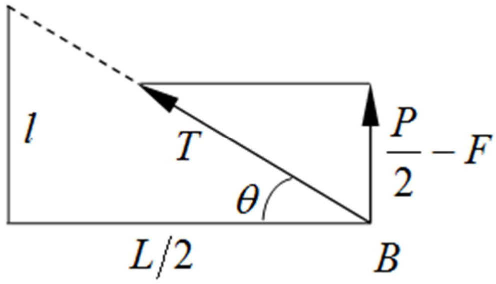

Fig. 3. *Force acting on the cable.*

On the other hand, as shown in Fig. 3, the upward tensile force $(\frac{P}{2}-F)$ acting on point B is a component of force produced by a cable, therefore

$$T\sin\theta=(\frac{P}{2}-F)=\frac{5}{3}F$$

Noting $\tan\theta=\frac{2l}{L}$ we obtain

$$T=\frac{5F}{3\sin\theta}=\frac{5F}{3}\sqrt{\frac{1+\tan^2\theta}{\tan^2\theta}}=\frac{5F}{3}\sqrt{\frac{1+(\frac{2l}{L})^2}{(\frac{2l}{L})^2}}=\frac{5FL}{6l}\sqrt{1+4(\frac{l}{L})^2}$$

thus

$$SE_0\left(\sqrt{1+4(\frac{l}{L})^2}-1\right)=\frac{5FL}{6l}\sqrt{1+4(\frac{l}{L})^2}$$

or

$$(6lSE_0-5FL)\sqrt{1+4(\frac{l}{L})^2}=6lSE_0$$

Since l/L is a very small quantity, using Taylor expansion $\sqrt{1+4(\frac{l}{L})^2}=1+2(\frac{l}{L})^2$ we have

$$(6lSE_0-5FL)(L^2+2l^2)=6lSE_0L^2$$

or

$$12SE_0l^3-10FLl^2-5FL^3=0$$

$$\frac{12SE_0}{5FL^3}-\frac{2}{L^2}\frac{1}{l}-(\frac{1}{l})^3=0$$

$$(\frac{1}{l})^3 + \frac{2}{L^2}\frac{1}{l} - \frac{12SE_0}{5FL^3} = 0$$

let $x = \frac{1}{l}$, $p = \frac{2}{L^2}$, $q = -\frac{12SE_0}{5FL^3}$, then the last equation can be written as

$$x^3 + px + q = 0$$

A unique real root of the last equation can be obtained by using Card an formula:

$$x_1 = \sqrt[3]{-\frac{q}{2} + \sqrt{(\frac{q}{2})^2 + (\frac{p}{3})^3}} + \sqrt[3]{-\frac{q}{2} - \sqrt{(\frac{q}{2})^2 + (\frac{p}{3})^3}}$$
$$= \sqrt[3]{\frac{6SE_0}{5FL^3} + \sqrt{(\frac{6SE_0}{5FL^3})^2 + (\frac{2}{3L^2})^3}} + \sqrt[3]{\frac{6SE_0}{5FL^3} - \sqrt{(\frac{6SE_0}{5FL^3})^2 + (\frac{2}{3L^2})^3}}$$

Finally, the protruded length of the screw is

$$l = \frac{1}{x_1}$$

5. Maximal Off Set of the Manipulator Arm

Let $p = 16F/3$ in Eq. (3), and taking the derivative of $y(x)$ with respect to x we get

$$y'(x) = \begin{cases} \frac{22F}{12EI}x^2 - \frac{FL}{EI}x & 0 \le x \le L/2 \\ -\frac{10F}{12EI}x^2 + \frac{5FL}{3EI}x - \frac{2FL^2}{3EI} & L/2 \le x \le L \end{cases}$$

Let $y'(x) = 0$ for $0 \le x \le L/2$ we have the following equation

$$\frac{22F}{12EI}x^2 - \frac{FL}{EI}x = 0$$

with whose two roots are $x_1 = 0$ and $x_2 = \frac{6L}{11}$. Since $y(0) = 0$, we only need to search for the second root. By noting $x_2 = \frac{6}{11}L > \frac{L}{2}$, it is enough to search for $x_2 = \frac{6L}{11}$ in the regions $0 < x \le L/2$.

For $L/2 \le x \le L$, let $y'(x) = 0$ we get

$$-\frac{10F}{12EI}x^2 + \frac{10FL}{6EI}x - \frac{2FL^2}{3EI} = 0$$

or

$$4x^2 - 10Lx + 4L^2 = 0$$

with two roots

$$x_{1,2} = \frac{10L \pm \sqrt{100L^2 - 80L^2}}{10} = (1 \pm \frac{\sqrt{5}}{5})L$$

But there is only a root $x_2 = (1 - \frac{\sqrt{5}}{5})L$ in the regions $L/2 \le x \le L$. Substituting $x_2 = (1 - \frac{\sqrt{5}}{5})L$ into the Eq. (3), we get the maximal offset of the manipulator arm

$$y((1-\frac{\sqrt{5}}{5})L) = \frac{FL^3}{18EI}[-5(1-\frac{\sqrt{5}}{5})^3 + 15(1-\frac{\sqrt{5}}{5})^2 - 12(1-\frac{\sqrt{5}}{5}) + 2]$$
$$= -\frac{\sqrt{5}FL^3}{45EI} \quad (5)$$

6. Analyse of the Vibration Suppression Effect

In order to investigate the vibration suppression effect of the device with its control algorithm, we will compare the maximal offset and the end-effector's offset of the manipulator with those in the case of without the device (or $P = 0$). In case of $P = 0$, as shown in Fig. 3, for $0 \le x \le L$, the bending moment $M(t)$ at distance x from the support A can be expressed as

$$M(x) = -F(L - x) = Fx - FL$$

By expressing the curvature as $\kappa = y''$ approximately y' , we have

$$Y'' = \frac{Fx - FL}{EI}$$

By using boundary conditions $Y(0) = 0$ and $Y'(0) = 0$, successive integrations of the last equation yields

$$Y(x) = \frac{Fx^3 - 3FLx^2}{6EI}$$

Thus the maximal offset of the manipulator is

$$Y(L) = \frac{FL^3 - 3FL^3}{6EI} = -\frac{FL^3}{3EI}$$

However from the Eq. (5) we know that in the case of using the device the maximal offset of the manipulator arm is

$$y((1-\frac{\sqrt{5}}{5})L) = -\frac{\sqrt{5}FL^3}{45EI}$$

and obtain

$$\frac{|Y(L)|}{|y((1-\sqrt{5}/5)L)|} = \frac{FL^3}{3EI} \Big/ (\frac{\sqrt{5}FL^3}{45EI}) = 3\sqrt{5}$$

The last equation means that the maximal offset of the manipulator in the case of without the device is $3\sqrt{5}$ times when compared with that in the case of without the device. Moreover, in the case of without the device the maximal offset of the manipulator appears at manipulator arm's end-effector. But in the case of using the device, the offset at manipulator arm's end-effector is zero, which is propitious to the accurate control of the manipulator's end-effector.

The above compare result shows that the device is certainly effective for the vibration suppression of manipulator.

7. Simulation

Suppose $L = 2m$, $F = 10N$, $EI = 6.6\times10^{10}$ N/m^2 $S = 10^{-4}m^2$, $P = 16F/3 = 160/3N$, $E_0 = 2\times10^{10}$ N/m^2 . Using the above the formula, we can obtain the protruded length of the screw $l = 0.0255m$. After regulating the protruded length of the screw according to the length, curve equation of the cantilever beam can be obtained through simulation operation. Its shape is shown in Fig. 4.

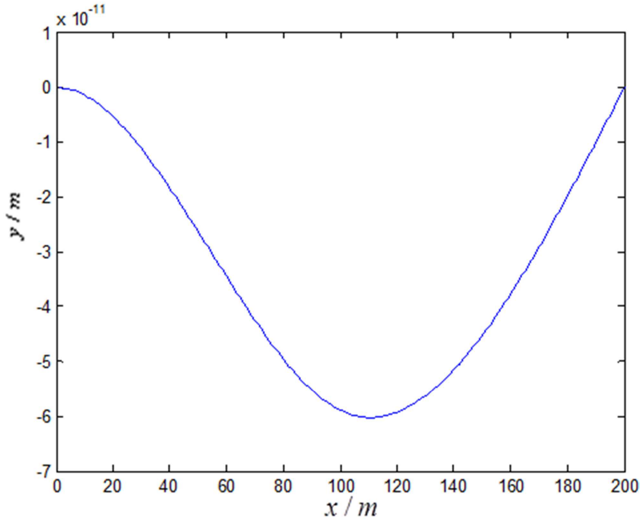

Fig. 4. *Shape of the cantilever beam.*

Fig.4 shows that the cantilever bends downwards at the left end and midpoint due to the action of the force F , which is consistent with the experimental result.

8. Conclusions

This paper deals with the vibration suppression problem of the manipulator arm with quadrate cross section. As long as the length of cross section is long enough compared to its breadth, we can consider that the manipulator arm bends only along breadth direction, and hence the bending moment can be counteracted by the tensile force of the cables. For general manipulator arm, we only need to use such two devices synchronously. But then for the convenience of computing component of forces and composition of forces, two devices have to be mounted in such a way that two screws are vertical mutually. In this case, as the component of the inertial force of load at manipulator arm's end-effector, shearing stress can be counteracted by the tensile forces from the two cables. However, since it is difficult for all of the two screws to be mounted on the middle part of the manipulator arm, there are some problems need to be investigated.

The distortion of the manipulator arm caused by its mass and acceleration is ignored in the paper for briefness and clarity. The reason is that in space application the manipulator arm is generally made of lightweight material, and its mass is much less than that of the load at manipulator arm's end-effector. On the other hand, the problem we deal with is the suppression of the vibration, but not the exhaustive elimination of the vibration. Even though the distortion caused by above causation is considered, protruded length of the screw can still be obtained according the approach introduced in the paper, to say the least.

Acknowledgement

This research is supported by the National Basic Research Program of China (Contract No. 2013CB733000)

References

[1] S. Marco, G. Paolo, M. Riccardo et al. Vibration control of a flexible space manipulator during on orbit operations. *Acta Astronautica*, 2012, 73(2): 109–121.

[2] S. B. Choi, C. C. Cheong, H. C. Shin. Sliding mode control of vibration in a single-link flexible arm with parameter variations. *Journal of Sound and Vibration*, 1995, 179(5): 737-48.

[3] V. G. Moudgal, K. M. Passino, S. Yurkovich. Rule-based control for a flexible-link robot. *IEEE Transactions on Control Systems Technology,* 1994, 2(4): 392-405.

[4] T. Yoshikawa, K. Hosoda. Modeling of flexible manipulators using virtual rigid links and passive joints. International Journal of Robotics Research, 1996, 15(3): 290-299.

[5] D. Economou, C. Mavroidis, I. Antoniadis. Robust vibration suppression in flexible systems using infinite impulse response digital filters. *Journal of guidance, control, and dynamics*, 2004, 27(2): 107–117.

[6] F. C. Edward, L. Javier. Use of piezoelectric actuators as elements of intelligent structures. *AIAA Journal*, 1987, 25(10): 1373-1385.

[7] S. Dong, K. M. James, S. Jinjun et al. A PZT actuator control of a single-link flexible manipulator based on linear velocity feedback and actuator placement. *Mechatronics*, 2004, 14 (4): 381-401.

[8] Y. Shengyuan, N. Bryan. Shape Control of beams by piezoelectric actuators. *AIAA Journal*, 2000, 38(12): 292-298.

[9] E. Augustyn, M. S. Kozien. A study on possibility to apply piezoelectric actuators for active reduction of torsional beams vibrations. *Acta Physica Polonica A*, 2014, 125(4): 164-168.

[10] V. Tvergaard, J. W. Hutchinson. Mode III effects on interface delamination. *Journal of the Mechanics and Physics of Solids*, 2008, 56(1): 215–229.

[11] J. W. Hutchinson. Delamination of compressed films on curved substrates. *Journal of the Mechanics and Physics of Solids,* 2001, 49(9): 1847-1864.

[12] H. M. Jensen, I. Sheinman. Numerical analysis of buckling-driven delamination. *International Journal of Solids and Structures*, 2002, 39(3): 3373-3386.

[13] C. N. Duong. A Unified approach to geometrically nonlinear analysis of tapered bonded joints and doublers. *International Journal of Solids and Structures*, 2006, 43(11): 3498-3526.

[14] M. G. James, J. G. Barry. Mechanics of Materials. Seventh edition, Toronto: Cengage Learning, 2009.

Biographies

An Kai An Kai received his PH.D. degree in control theory and control engineering from Xi'an Jiaotong University, Xi'an, China, in 2000. He has published more than 100 conference and journal papers, and his more than 30 invention has been patented. His research interests include intelligent control, optical engineering, and space robot.